Atomic positions around misfit dislocations on a planar heterointerface

R. Bonnet and M. Loubradou
Institut National Polytechnique de Grenoble, Laboratoire de Thermodynamique et Physico-Chimie Métallurgiques (URA 29)/Ecole Nationale Supérieure d'Electrochimie et d'Electrométallurgie de Grenoble, Domaine Universitaire, Boîte Postale 75, 38402 Saint Martin-d'Heres, France
(Received 3 February 1994)

An approach describing the atomic positions around misfit dislocations lying along a planar interface is presented using both discrete (the atomic structural unit repeating along the interface) and continuous (anisotropic elasticity of heterogeneous media) information. An appropriate computer program illustrates the usefulness of the method when applied to high-resolution electron-microscopy images of the (001) CdTe/(001)GaAs and (1 $\bar{1}$ $\bar{1}$) Au/(001)Au interfaces. Potentially, any two crystal structures can be taken into account.

I. INTRODUCTION

Many properties of polycrystals and heterostructures built for microelectronic devices depend on the dislocation densities along the interfaces, which explains why a number of papers, e.g., Refs. 1, 2, and 3, are devoted to the observation of crystalline interfaces by conventional or high-resolution electron microscopy (HREM). As a matter of fact, despite an immense number of HREM images presented in the literature, our ability to model reasonably well the atomic site positions in the interfacial region remains drastically limited when defects are present. For grain boundaries in cubic materials, atomic relaxation simulations are, however, in progress and can sometimes give information on the local displacement field near linear singularities, e.g., Refs. 4 and 5. For heterointerfaces, pseudogeometric models are rather used to describe the epitaxial orientation relationships, e.g., Refs. 6–9. In some recent works,[10–15] the atomic structures of heterointerfaces separating cubic crystals have been investigated using atomic relaxation procedures. In all these works, the two crystals have parallel ⟨100⟩ directions and the interface is parallel to a common (001) or (110) plane. All these methods can be called *discrete approaches* to the structures of interfaces because they give a way to determine the atomic positions inside an atom box including a part of each crystal. Applications to low-symmetry crystal lattices and more complex orientation relationships are not yet considered because of the difficulty in describing the complex interactions between several kinds of atoms and the requirement to ensure stability of each crystalline structure. Other limitations require us to reduce the size of the atom box to save prohibitive calculation time, i.e., require high lattice misfits and the need to approximate the lattice misfits by rational fractions.

II. THEORY

Another approach to determine the atomic structures around misfit dislocations lying along a planar interface separating any two crystals is presented below. It is based on two assumptions.

(i) The lattice misfits are accommodated by elastically deformed atomic structural units repeating along the interface, as in Ref 16: forces are transmitted across the interface; between two dislocation cores, to accommodate the misfit, the discontinuity $\Delta\mathbf{u}$ of the displacements changes linearly and is zero in the medium point.

(ii) The displacement field $\mathbf{u}$ is periodic and follows the heterogeneous anisotropic elasticity theory as expressed in Ref. 17 for intrinsic dislocations. Far from the interface, both crystals remain undeformed.

Because of the use of an elastic continuum, this method is called the *continuous approach*. Two examples will illustrate the method at atomic scale, the (001)CdTe/(001)GaAs heterojunction and the (1 $\bar{1}$ $\bar{1}$) Au/(001) Au grain boundary facet, from HREM images observed in Refs. 18 and 19.

Before presenting these examples, it is of interest to review briefly results obtained from the discrete approaches, for which some comparisons with macroscopic measurements could be performed.

In Refs. 11 and 12, the simplification is made of a perfect match between eight lattice units of the Ag crystal and nine lattice units of the Cu crystal. Embedded atom method functions are used in Monte Carlo simulation to model the interatomic interaction at (001)Ag/(001)Cu heterointerfaces. The atom boxes involve 2755 atoms. An approximate correlation between calculated equilibrium profiles has been made from Auger intensity profiles through the interface. However, the obtained displacement field was not discussed.

In Ref. 15, the assumption is made of a perfect match between 15 lattice units of the GaAs substrate and 14 lattice units of the GaSb epilayer. The (001)GaAs/(001)GaSb interface is constructed from atomic relaxations of an atom box containing about 15 000 atoms, using the Keating potential and boundary conditions given by the heterogeneous isotropic elasticity theory.[20] Two cases are investigated, cf. their Figs. 2(a) and 2(c). The first involves a planar interface, the second a slightly corrugated interface involving two monolayers. This second model was proved to be in better agreement with their x-ray-diffraction experiments. At this point, it is interesting to note that, forgetting the chemistry of the atomic

sites, all their obtained displacement fields were not differing substantially [see their Figs. 2(a), 2(b), and 2(c)], as easy to prove from superimpositions. The idea arises then to test if the continuous approach from heterogeneous elasticity can be a valid tool to describe the positions of atomic columns in the vicinity of misfit dislocations visible in HREM.

Before presenting results, it is useful to summarize some symbols and to describe briefly the successive numerical steps leading to the atomic representation. If the two matching lengths are denoted L_1 and L_2 for crystal 1 and 2, respectively, the period is $T=L_1L_2/(L_2-L_1)$. Defining the misfit by $\varepsilon=2(L_2-L_1)/(L_1+L_2)$ leads to the Burgers vector modulus $b=\varepsilon T=2L_1L_2/(L_1+L_2)$.

The first calculation step concerns the initial state of the two crystals. The question is to assemble two stress-free crystals for which the atomic structural unit is correctly described in a point C of the interface, chosen as the middle point between two dislocation cores. In practice, the atomic column positions of both crystals are determined around C by multislice calculations of the image contrast. The route followed to describe the relative position of the two crystals is the following. For each crystal, the internal coordinates (α_1,α_2) of C in a two-dimensional cell perpendicular to the projection direction are measured. For our two examples, this cell has base vectors that are chosen (arbitrarily) as the projections of the vectors (**c**-**a**) and (**c**-**b**). The usefulness of this pair (α_1,α_2) is both to position the two crystals relative to each other and to place the interface inside the unit cells of the crystals.[16]

The second step is to calculate the displacement vector **u** of each atom and to determine the final atomic column positions in the projection plane. Formula (34a) in Ref. 17 can be used if the anisotropic elastic constants are known. Another possibility is to use the approximation of the heterogeneous isotropic elasticity theory,[20] as already applied in Ref. 15, for which the formulas can be written in a much more simplified form. However, care must be taken on the determination of the shear modulus μ and Poisson ratio ν of each crystal from its constants C_{ijkl}, see Appendix 2 in Ref. 21. In the Cartesian frame of Ref. 20 and remembering that an appropriate symbol $+$ or $-$ is attached to each medium considered, the three components of **u** are

$$u_1=b_1[-\mathrm{sgn}(x_2)/\pi][K+L(3-4\nu)]F_6 +[Kb_2F_5/\pi]+2L[b_1x_2F_2+|x_2|b_2F_1]/T\ , \tag{1}$$

$$u_2=b_2[-\mathrm{sgn}(x_2)/\pi][K+L(3-4\nu)]F_6 -[Kb_1F_5/\pi]+2L[-b_2x_2F_2+|x_2|b_1F_1]/T\ , \tag{2}$$

$$u_3=b_3[-\mathrm{sgn}(x_2)S/(\pi\mu)]F_6\ , \tag{3}$$

where T is the period, $\mathrm{sgn}(x_2)=-1$ if $x_2<0$ or $+1$ if $x_2>0$, and

$$K^+=K^-=[1-L^-(3-4\nu^-)+L^+(3-4\nu^+)],\quad S^+=S^-=\mu^+\mu^-/(\mu^-+\mu^+)\ , \tag{4}$$

$$L^+=\mu^-/[\mu^++\mu^-(3-4\nu^+)]\ ;\quad L^-=\mu^+/[\mu^-+\mu^+(3-4\nu^-)]\ , \tag{5}$$

$$F_1=(\tfrac{1}{2})\left[\frac{\sinh(2\pi|x_2|/T)}{\cosh(2\pi|x_2|/T)-\cos(2\pi x_1/T)}-1\right]\ , \tag{6}$$

$$F_2=(\tfrac{1}{2})\frac{\sin(2\pi x_1/T)}{\cosh(2\pi|x_2|/T)-\cos(2\pi x_1/T)}\ , \tag{7}$$

$$F_5=(-\tfrac{1}{2})\log\{1-2[\cos(2\pi x_1/T)]\exp(-2\pi|x_2|/T) +\exp(-4\pi|x_2|/T)\}\ , \tag{8}$$

$$F_6=\arctan\left[\frac{\sin(2\pi x_1/T)}{\exp(2\pi|x_2|/T)-\cos(2\pi x_1/T)}\right]\ . \tag{9}$$

For the two examples treated below, calculations show that anisotropic elasticity effects are small, except very close to the dislocation cores where differences in **u** can reach a few hundredths of a nanometer. Theoretical images have been computed using the Electron Microscope Software (EMS) package[22] to locate precisely the atomic column positions in the experimental images.

III. CALCULATIONS AND RESULTS

The (001) CdTe/(001) GaAs heterojunction described in Ref. 18. The crystals were found to be free of long-range stresses after vacuum annealing at 600 °C for 100 h in an evacuated ampule with 10–5 Torr pressure. The lattice parameters of CdTe and GaAs are, respectively, 0.6481 and 0.5653 nm.[23] The interface contains Lomer misfit dislocations running along the common projection direction [110]. The structural units match two vectors $\frac{1}{2}[1\bar{1}0]$. As a result, $T=3.13$ nm, which corresponds well to the measured period. As defined above, the misfit is $\varepsilon=13.6\%$ and $b=0.427$ nm. Undeformed crystal images have been computed to identify the atomic column positions far from the dislocation cores using a defocus close to the Scherzer defocus (for the used JEOL 400-kV microscope) and thicknesses less than a period T. They show that the atomic column positions are separated by white dots. The atomic structural unit close to the medium point C between two dislocation cores has then been determined assuming that the white dots separate the atomic columns [Fig. 1(a)], which was checked subsequently by multislice computations. From measurements, for both CdTe and GaAs, the structural units are such that $\alpha_1=\frac{1}{5}$, $\alpha_2=\frac{1}{5}$. Both crystals are rather elastically anisotropic. For GaAs (in GPa), $C_{11}=118$, $C_{12}=53.5$, $C_{44}=59.4$,[24] with a Zener coefficient[25] $A=2C_{44}/(C_{11}-C_{12})=1.84$. For CdTe (in GPa), $C_{11}=53.5$, $C_{12}=36.9$, $C_{44}=20.2$,[24] with $A=2.43$. Figure 1(a) represents the calculated positions of the atomic columns around the misfit dislocations. An idea of the dislocation core region is given by the mushroom-shape dotted curve. This curve is derived from application of **u** along a circle of radius b drawn in the initial stress-free state. Figure 1(b) shows the positions of the theoretical atomic column positions (black small crosses) superimposed on the experimental image. Figure 1(c) represents

the theoretical image of the heterojunction using an atom box of 704 atoms whose positions correspond exactly to those indicated in Fig. 1(a). Superimposing the theoretical atomic columns drawn in Figs. 1(b) and 1(c) shows indeed that the experimental and theoretical white dots are placed almost identically, except in the dislocation cores, which means that the continuous approach succeeds to predict the observed surrounding displacement field. Note that in these calculations, free-surface relaxations of the dislocations have been neglected. They are known to be small for edge dislocations running perpendicular to the foil.[26]

Extra calculations have been performed to test the assumption of a displacement field resulting from the presence of translation Volterra dislocations rather than intrinsic dislocations. Indeed, the result proves to be quite negative. The new limiting boundary conditions differ only by the point that now $\Delta\mathbf{u}$ must be a staircase function with discontinuities $\mathbf{b}$ at the dislocation cores.[17,20] This condition cannot preserve the atomic structural units since first, $\mathbf{u}$ is not periodic with T and second, the length misfit is not gradually taken into account. Figure 2 gives an idea of the discrepancy between the two approaches: the atomic positions are indicated in filled or

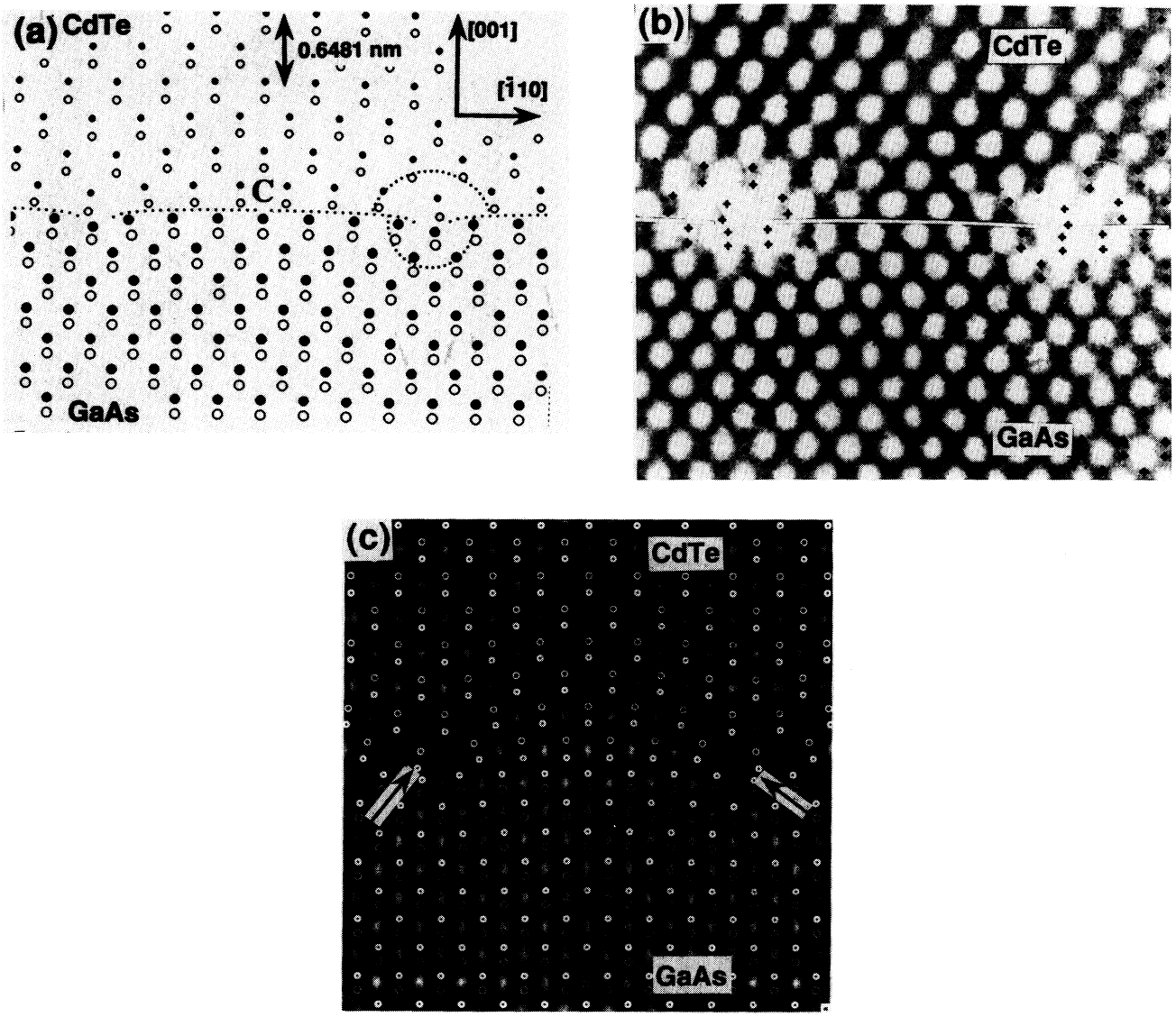

FIG. 1. (001)CdTe/(001)GaAs heterojunction: (a) atomic column positions predicted from Eq. (34a) in Ref. 17. They are differentiated by four symbols. The interface is indicated in dotted line. C is the medium point between two dislocation cores. The mushroomlike curve encloses a misfit dislocation core. (b) HREM image from Ref. 18. Good agreement between the experimental positions of the atomic columns (gray dots) and their theoretical positions (small black crosses), except in the dislocation cores. (c) Theoretical image of the heterojunction computed with a box of 704 atoms. Two dislocation cores are indicated with arrows. Data: defocus= -35 nm; thickness = 2.7 nm; Cs=1.1 nm; spread of focus=10 nm; semiangle of convergence=0.8 mrad; Debye-Waller coefficients=0.005 nm^2; atomic absorption: Cd, Te=0.07; Ga, As=0.05.

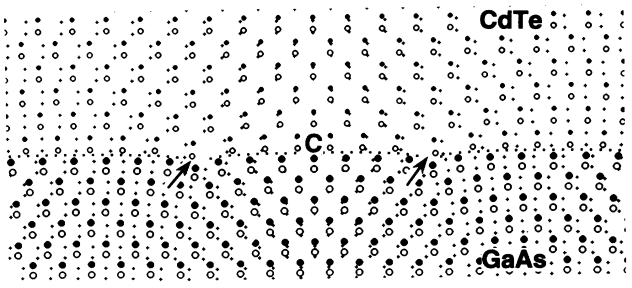

FIG. 2. Atomic positions in the vicinity of the dislocations (arrows) as calculated from the Volterra approach (small crosses) and ours [see, also, Fig. 1(a)]. The discrepancy between the two descriptions increases continuously from the medium point *C*. On the left and right, atomic structural units are not preserved with the Volterra approach.

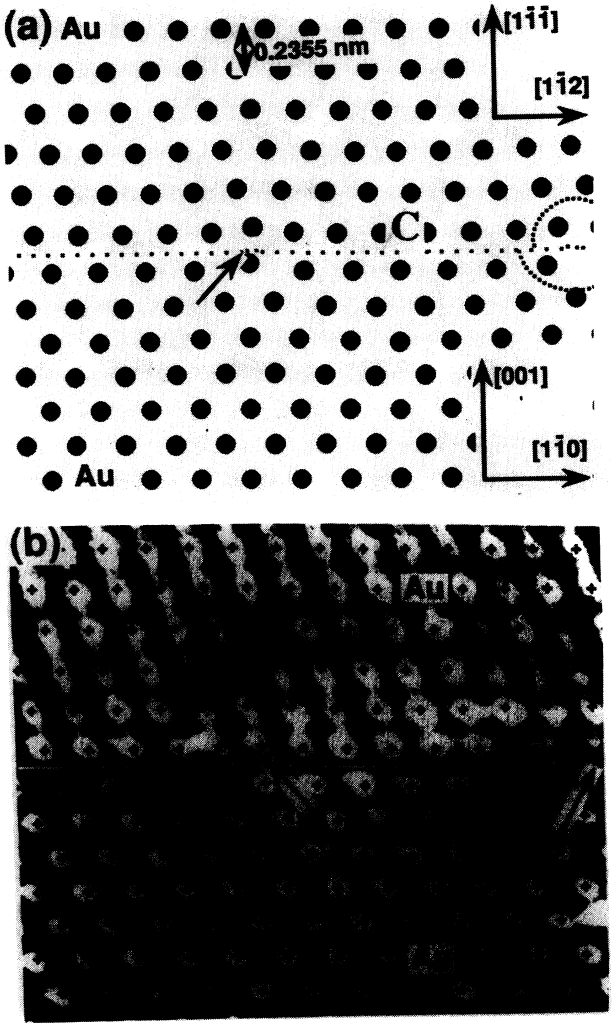

FIG. 3. Grain boundary facet in gold. Arrows indicate misfit dislocation cores. (a) Predicted atomic column positions. The interface is indicated in dotted line. An idea of the dislocation core region is given by the mushroom-shape dotted curve. (b) HREM image from Ref. 19. Good agreement between the experimental positions of the atomic columns (white dots) and their theoretical positions (small black crosses).

empty circles with our description, while they are indicated by small black crosses with the Volterra description. The departure between the two kinds of positions is observed to increase continuously with the distance from *C*. Finally, multislice calculations of an atom box including the interface (724 atoms) have been undertaken, confirming a total disagreement between the experimen-

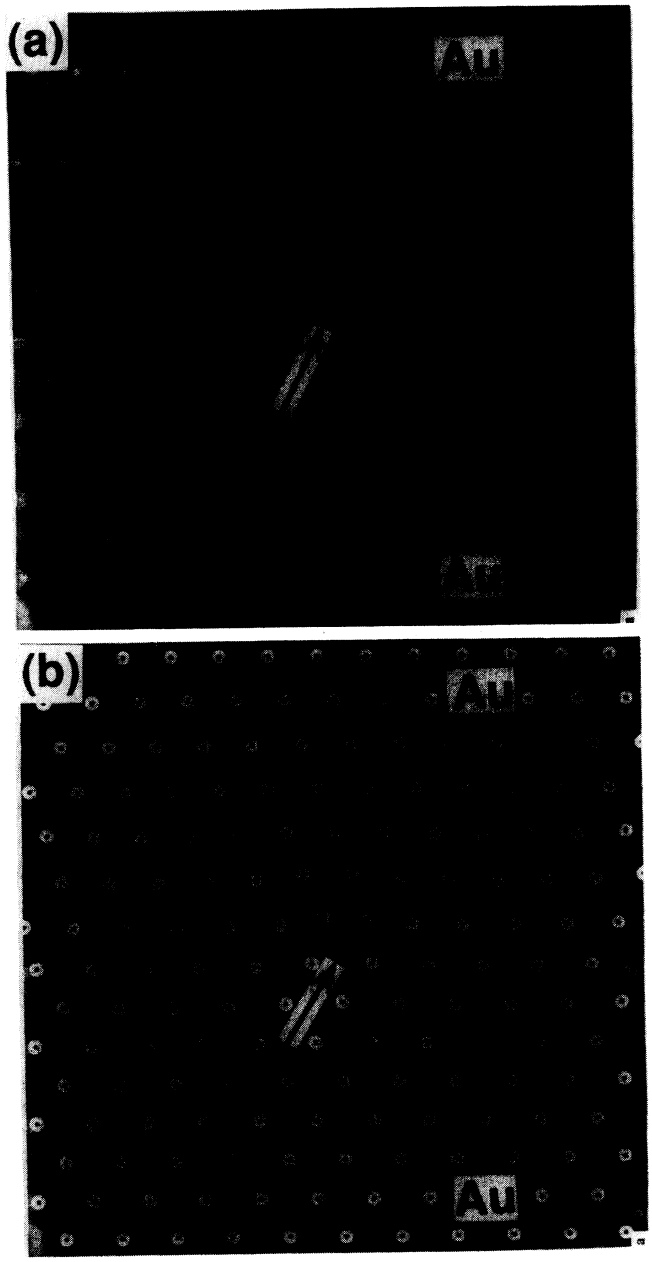

FIG. 4. (a) and (b): (1$\bar{1}$ $\bar{1}$)Au/(001)Au grain-boundary facet. Calculated images of the grain boundary. Theoretical image computed with a box of 358 atoms. Data: defocus = −50 nm; thickness = 2.5 nm; Cs = 1.05 nm; spread of focus = 9 nm; semi-angle of convergence = 0.7 mrad; Debye-Waller coefficient = 0.003; atomic absorption = 0.09. The arrows indicate misfit dislocation cores. (a) Calculated image. (b) Atomic column positions superimposed on the image in (a). Except close to the edges of the image, white dots represent the atomic column positions.

tal image and the calculated image assuming the Volterra approach.

The $(1\bar{1}\,\bar{1})$*Au/(001) Au grain boundary in Ref. 19.* Unusual misfit dislocations have been observed along grain-boundary facets in gold.[19,27] They are associated with quasiperiodic grain-boundary structures, e.g., the $(1\bar{1}\,\bar{1})$Au/(001)Au facet in Ref. 19 treated below. The dislocations run along a common direction $\langle 110\rangle$. The lattice parameter of gold is $a=0.40783$ nm.[28] Between two dislocation cores, the atomic structural units elastically deform to match two vectors, $\frac{1}{4}[1\bar{1}2]$ of the upper grain and $\frac{1}{2}[1\bar{1}0]$ of the lower grain. This means that $T=a\sqrt{6}/(4-2\sqrt{3})=1.86$ nm, $\varepsilon=(4-2\sqrt{3})/(2+\sqrt{3})=14.4\%$, and $b=0.268$ nm. Undeformed crystal images have been computed to locate the atomic column positions in the image. In particular, the Scherzer defocus (for the used JEOL 400-kV microscope) has been inserted in the data. A small range of foil thicknesses, around 2.5 nm, has been found possible to fit the theoretical and experimental contrasts. As a result, in the image, the white dots represent the atomic column positions. The structural unit close to *C*, Fig. 3(a), is such that for the upper crystal $\alpha_1=\frac{1}{4}$, $\alpha_2=\frac{1}{4}$, while for the lower crystal $\alpha_1=\frac{1}{4}$, $\alpha_2=0$. In the region marked *C*, the structural unit ensures the alignment of (001) atomic planes of the upper crystal with $(1\bar{1}\,\bar{1})$ atomic planes of the lower crystal. Gold is elastically anisotropic since (in GPa) $C_{11}=186$, $C_{12}=157$, $C_{44}=42$, with $A=2.9$.[25] The deformation around the Lomer edge misfit dislocations is represented in Fig. 3(a). Figure 3(b) illustrates the reasonable match of the theoretical (small black crosses) and experimental positions (in white) of the atomic columns. The fact that the white dots represent still the atomic positions along the deformed grain-boundary facet is shown in Figs. 4(a) and 4(b), using a box of 358 atoms. In these images, deleterious edge effects are due to the nonperiodicity of the atom box.

IV. CONCLUSION

As shown above, the continuous approach can reasonably account for the experimental displacement fields in the vicinity of misfit edge dislocations observed along the (001) CdTe/(001) GaAs heterojunction and the $(1\bar{1}\,\bar{1})$Au/(001) Au grain-boundary facet, except of course in the very cores of the defects. Our result confirm the mathematical descriptions given in Refs. 17 and 20 and, in particular, that the limiting boundary conditions chosen are meaningful. Note that the match with an experimental image could possibly be obtained from the discrete approach but, because an elastic problem has a unique solution,[29] this would imply other limiting boundary conditions necessarily very close to ours. On the other hand, treating the atomic interactions of four different kinds of atoms interacting in the interfacial region seems intractable by current potential models.

In addition, it has been shown that a simple Volterra description of the misfit dislocations is quite unable to account for the experimental atomic column positions. The inadequacy results from the fact that (i) the misfit is not accommodated gradually along the interface and (ii) the **u** field is not periodic. In addition, such a description would be associated to unprobable long-range stresses[17,25] in the annealed specimens.

If the crystallography of the heterointerface is simple enough, atomic relaxation procedures can benefit by our method to reduce the size of the needed atom boxes. Nonparallelepipedic atom boxes could also be constructed for biperiodic heterointerfaces starting from boundary conditions specified for hexagonal networks of misfit dislocations.[30] For more complicated heterointerfaces, involving, for instance, low-symmetry crystals for which atomic relaxation procedures are not yet available, our approach is apparently unique to provide a reasonable estimate of the atomic positions around misfit dislocations.

ACKNOWLEDGMENTS

Dr. K. L. Merkle from Argonne National Laboratory (IL) and Dr. A. F. Schwartzman from Stanford University (CA) are gratefully acknowledged for providing the HREM images shown in Fig. 1(b) and Fig. 3(b). The Institut National Polytechnique de Grenoble is "Unité Associée au Centre National de la Recherche Scientifique No. 29."

[1] *Epitaxy of Semiconductor Layered Structures,* edited by R. T. Tung, L. R. Dawson, and R. L. Gunshor, MRS Symposia Proceedings No. 183 (Materials Research Society, Pittsburgh, 1990).

[2] *Strain Relaxation in Epitaxial Films* [J. Electron. Mater. **20**, 805 (1991)].

[3] *Structure and Properties of Interfaces in Materials,* edited by W. A. T. Clark, U. Dahmen, and C. L. Briant, MRS Symposia Proceedings No. 238 (Materials Research Society, Pittsburgh, 1992).

[4] A. P. Sutton and V. Vitek, Philos. Trans. R. Soc. London, Ser. A **309**, 1 (1983).

[5] J. Th. M. De Hosson and V. Vitek, Philos. Mag. A **61**, 305 (1990).

[6] W. Bollmann, *Crystal Defects and Crystalline Interfaces* (Springer-Verlag, Berlin, 1970); *Crystal Lattices, Interfaces, Matrices,* edited by W. Bollmann (Pinchat, Geneva, 1982).

[7] R. Bonnet and F. Durand, Philos. Mag. **32**, 557 (1975).

[8] U. Dahmen, Acta Metall. **30**, 63 (1982).

[9] A. Catana, J.-P. Locquet, S. M. Paik, and I. Schuller, Phys. Rev. B **46**, 15 477 (1992).

[10] C. C. Matthai and P. Ashu, *Intergranular and Interphase Boundaries, Colloque, Paris, 1989* [J. Phys. (Paris) Colloq. **51**, C1-873 (1990)].

[11] P. Wynblatt and S. A. Dregia, *Intergranular and Interphase Boundaries* (Ref. 10), p. C1-757.

[12] J. P. Rogers III, P. Wynblatt, S. M. Foiles, and M. I. Baskes, Acta Metall. Mater. **38**, 177 (1990).

[13] U. Wolf, S. M. Foiles, and H. F. Fischmeister, Acta Metall. Mater. **39**, 373 (1991).

[14] P. Gumbsch, M. S. Daw, S. M. Foiles, and H. F. Fischmeister, Phys. Rev. B **43**, 13 833 (1991).

[15] A. Bourret and P. H. Fuoss, Appl. Phys. Lett. **61**, 1034 (1992).

[16] R. Bonnet and M. Loubradou, in *Structure and Properties of*

Interfaces in Materials (Ref. 3), p. 29.
[17]R. Bonnet, Acta Metall. **29**, 437 (1981).
[18]A. F. Schwartzman and R. Sinclair, J. Electron. Mater. **20**, 805 (1991).
[19]K. L. Merkle, Ultramicroscopy **37**, 130 (1991); *Intergranular and Interphase Boundaries* (Ref. 10), p. C1-251.
[20]R. Bonnet, Philos. Mag. A **43**, 1165 (1981).
[21]R. Bonnet and A. J. Morton, Philos. Mag. A **56**, 815 (1987).
[22]P. Stadelmann, Ultramicroscopy **21**, 131 (1987).
[23]P. Villars and L. D. Calvert, *Pearson's Handbook of Crystallographic Data for Intermetallic Phases* (ASM, Metals Park, Ohio, 1985), Vol. 3, p. 2555.
[24]R. F. S. Hearmon, in *Numerical Data and Functional Relationships in Science and Technology,* edited by K. H. Hellwege and A. M. Hellwege, Landolt-Börnstein, New Series, Vol. 11, Pt. 1.2.1 (Springer-Verlag, Berlin, 1979), pp. 26 and 27.
[25]J. P. Hirth and J. Lothe, *Theory of Dislocations,* 2nd ed. (Wiley, New York, 1982), p. 837.
[26]J. D. Eshelby and A. N. Stroh, Philos. Mag. **42**, 1401 (1951).
[27]W. Krakow and D. A. Smith, J. Mater. Res. **1**, 47 (1986).
[28]B. D. Cullity, *Elements of X-ray Diffraction,* 2nd ed. (Addison-Wesley, Reading, MA, 1978), p. 507.
[29]J. Mandel, *Cours de Mécanique des Milieux Continus-II* (Gauthier-Villars, Paris, 1966), p. 660.
[30]A. Bouzaher and R. Bonnet, Acta Metall. Mater. **41**, 1595 (1993); Philos. Mag. A **66**, 823 (1992); Phys. Status Solidi B **181**, 117 (1994).

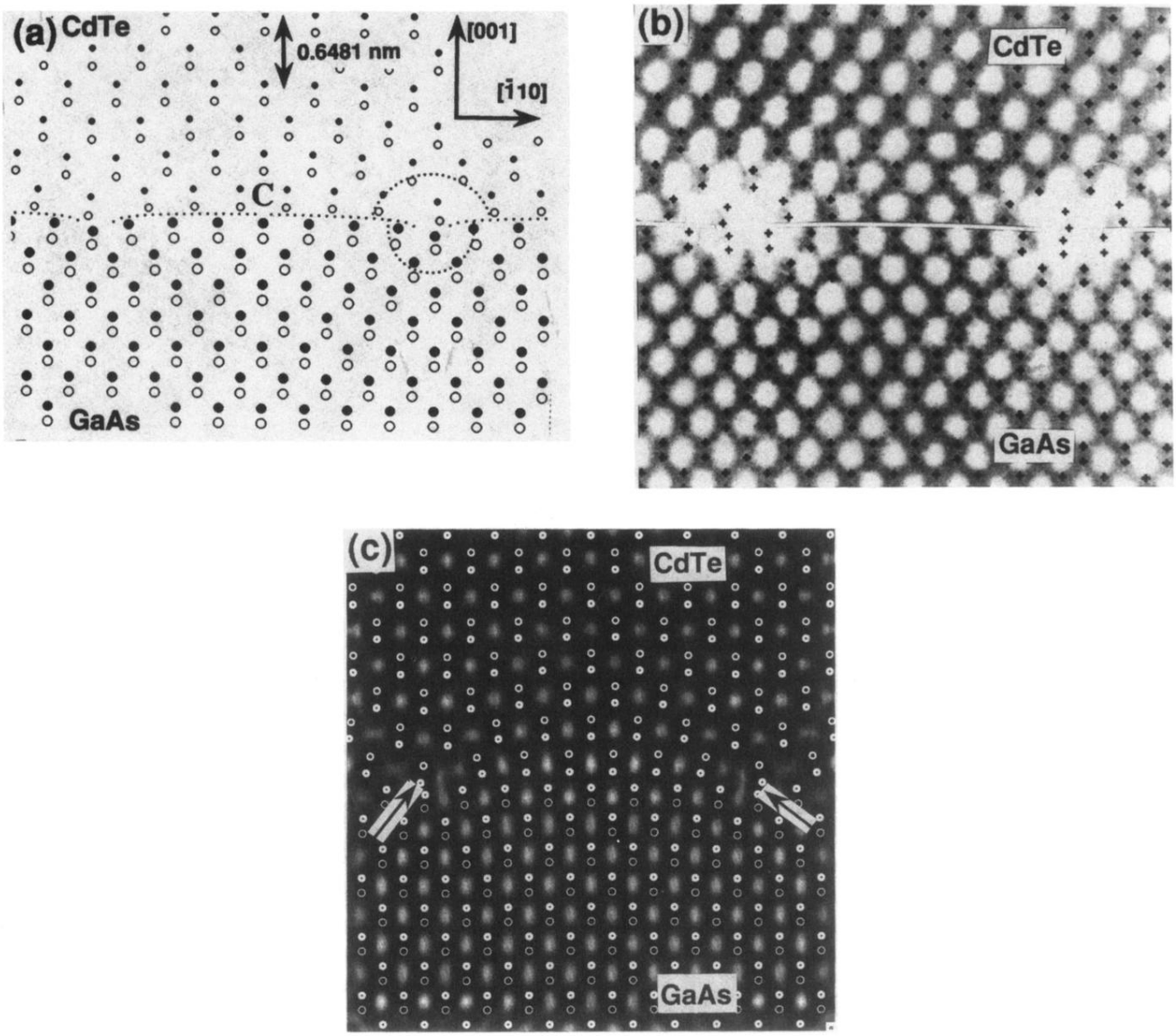

FIG. 1. (001)CdTe/(001)GaAs heterojunction: (a) atomic column positions predicted from Eq. (34a) in Ref. 17. They are differentiated by four symbols. The interface is indicated in dotted line. *C* is the medium point between two dislocation cores. The mushroomlike curve encloses a misfit dislocation core. (b) HREM image from Ref. 18. Good agreement between the experimental positions of the atomic columns (gray dots) and their theoretical positions (small black crosses), except in the dislocation cores. (c) Theoretical image of the heterojunction computed with a box of 704 atoms. Two dislocation cores are indicated with arrows. Data: defocus= −35 nm; thickness = 2.7 nm; Cs=1.1 nm; spread of focus=10 nm; semiangle of convergence=0.8 mrad; Debye-Waller coefficients=0.005 nm^2; atomic absorption: Cd, Te=0.07; Ga, As=0.05.

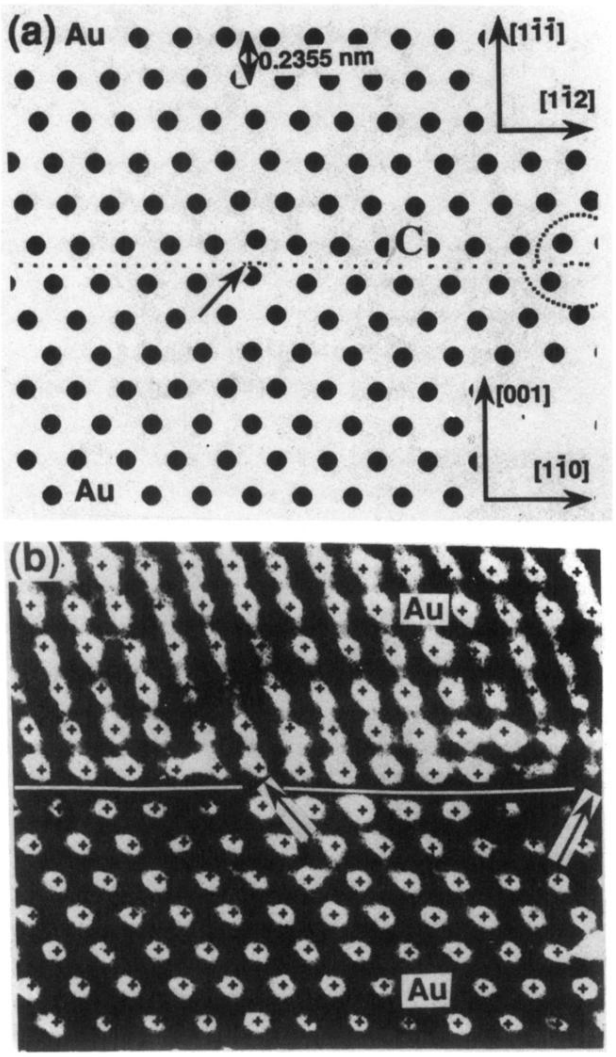

FIG. 3. Grain boundary facet in gold. Arrows indicate misfit dislocation cores. (a) Predicted atomic column positions. The interface is indicated in dotted line. An idea of the dislocation core region is given by the mushroom-shape dotted curve. (b) HREM image from Ref. 19. Good agreement between the experimental positions of the atomic columns (white dots) and their theoretical positions (small black crosses).

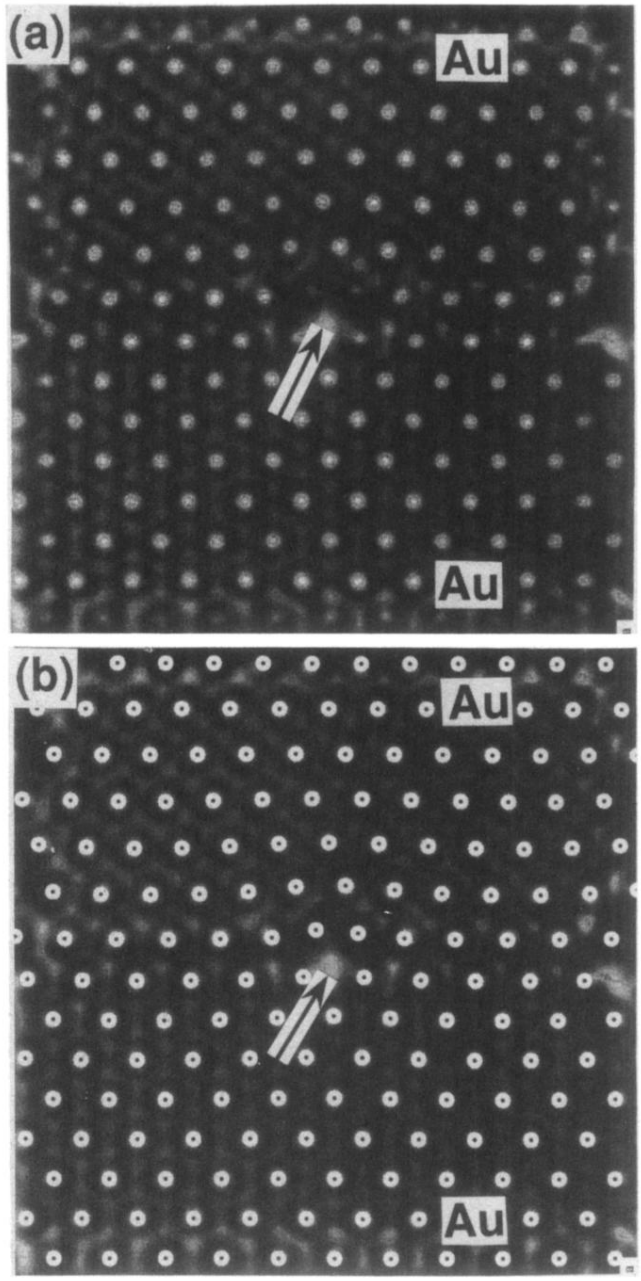

FIG. 4. (a) and (b): $(1\bar{1}\,\bar{1})$Au/(001)Au grain-boundary facet. Calculated images of the grain boundary. Theoretical image computed with a box of 358 atoms. Data: defocus $= -50$ nm; thickness $= 2.5$ nm; Cs $= 1.05$ nm; spread of focus $= 9$ nm; semi-angle of convergence $= 0.7$ mrad; Debye-Waller coefficient $= 0.003$; atomic absorption $= 0.09$. The arrows indicate misfit dislocation cores. (a) Calculated image. (b) Atomic column positions superimposed on the image in (a). Except close to the edges of the image, white dots represent the atomic column positions.